APPLICATION OF NUMERICAL METHODS FOR COMPUTATION OF THE ABEL INTEGRAL EQUATION TO SPECTROSCOPIC DATA[1)]

SEMBER, V.,[2)] Praha

A comparison of six numerical methods for computing the Abel transformation is presented. The dependence of accuracy of each method on the number of data points and experimental errors for two typical types of radial intensity distribution is shown. An application of suitable methods to the computation of rotational temperature from an OH molecule vibrational band is discussed.

I. INTRODUCTION

In plasma spectroscopy, the line of sight of the external intensity $I(y)$ of an optically thin cylindrical plasma is related to the radial intensity $i(r)$ through the Abel integral equation and its inverse [1]

$$I(y) = 2\int_y^R \frac{r\,i(r)}{(r^2-y^2)^{1/2}}\mathrm{dr} \tag{1}$$

$$i(r) = \frac{-1}{\pi}\int_r^R \frac{I\prime(y)}{(y^2-r^2)^{1/2}}\mathrm{dy} \tag{2}$$

where $I(y)'$ is the first derivative of the side-on intensity with respect to the lateral coordinate y, and R is the over-all radius of the plasma column.

To obtain the radial distribution $i(r)$ from a set of experimantal values of $I(y_i)$ $(i = 1,\ldots,N)$, one must either solve the integral equation (1) or evaluate Eq. (2). The direct computation of the Eq. (2) involves numerical differentiation which results in a considerable amplification of the experimental errors. To avoid this numerical difficulty, a large number of techniques have been devised. Conventional methods may be divided into two classes: Numerical techniques and Analytical approximation methods.

In numerical techniques (for example [2]), either the side-on intensity or the radial intensity is assumed to have a variation given by a particular law over each interval y_i. The recurrence formula for $i(r)$ is used, the computation starts at the outer radius. Numerical techniques are very simple and quick, howerer, numerically unstable with respect to the error propagation.

Analytical approximation methods are based either on approximation or on interpolation $I(y_i)$ with some orthogonal series expansions with least-square fitting or with some spline functions, then $i(r)$ is obtained from Eq. (2) analytically or numerically [1,3,4]. To avoid differentiation entirely a derivative-free formula was derived from Eq. (2) [5,6], which is less sensitive to the experimental errors. The interpolation techniques require, however, a prior smothing of experimental data, the approximation methods, on the other hand, are usually rather complicated and involve some numerical difficulties.

Recently several new numerical methods have been developed which seem to be numerically stable and have no disadvantages of conventional ones [7-9]. Some of these methods are devised on the assumption that a high-speed computer is available, and a new explicit solution of Eq. (1) is derived [9], which enables very accurate numerical computation for a very wide range of side-on intensity functions. In other cases emphasis is put on the capability of handling large data sets [10].

II. NUMERICAL METHODS

1. Frie's method

Radial intensity is assumed to be replaced, over a small interval y_i again, by a second-degree interpolation formula, which is substituted into Eq. (1). The simple recursive relation for the radial intensitz is derived [1, 2].

2. Cubic spline method

Experimental data are interpolated by means of cubic spline polynomials, the analytical solution of Eq. (2), in each interval y^i, is obtained [3]. A cubic spline algorithm was taken from [10].

[1)] Contribution presented at the 8th Symposium on Elementary Processes and Chemical Reactions in Low Temperature Plasma, STARÁ LESNÁ, May 28-June 1, 1990

[2)] Institute of Plasma Physics, Czechosl. Acad. Sci., Pod vodárenskou věží 4, 182 11 PRAHA 8, CSFR

3. Cremers' method

The method is based on dividing the data $I(y_i)$ into a number of segments, then a least-squares polynominal is fitted to each segment so that Eq. (2) can be integrated exactly. Since the fitted curve must have zero slope at the centre, a polynomial in x^2 is used for the data subset nearest to $y = 0$ [1]. In our case, the number of segments was being chosen up to five on condition that the minimum of data points in each segment was five. The least-squares polynomial of fourth degree was then fitted to each segment plus three points from each of the adjacent segments, with the exception of the extreme segments.

4. The Vicharelli and Lapatovich method.

The principle of this method is taken from deconvolution techniques [7]. Following Vicharelli and Lapatovich we define the mean radial intensity.

$$\bar{i}(y) = I(y)/2x_0(y),$$

where $x_0(y) = (R^2 - y^2)^{1/2}$, so that Eq. (1) can be rearranged as

$$\bar{i}(y) = \int_0^R i(r)g(r,y)\mathrm{d}r, \tag{3}$$

where

$$\begin{aligned} g(r,y) &= 0 && 0 \le r < y \\ g(r,y) &= r/\left[(r^2 - y^2)^{1/2} x_0(y)\right] && y \le r \le R \end{aligned}$$

The iterative algorithm for computing $i(r)$ is used. The mean values of the experimental data $I(y_i)$ are used as the first approximation. An improved estimate is calculated from

$$i_j = i_{j-1}(r_i) + [I(y_i)/2x_0(y_i) - \bar{i}_{j-1}(r_i)],$$

where $\bar{i}_{j-i}(r_i)$ by Eq. 3 using the $(j-1)$ the estimate of $i(r)$.

5. The Tatum and Jaworski method.

The explicit solution of Eq. (1) has been offered in paper [8]:

$$i(\varrho) = -\frac{1}{\pi R\varrho}\frac{\mathrm{d}}{\mathrm{d}\varrho}\left\{(1-\varrho^2)^{1/2}\int_0^{\pi/2} I\left[(\cos^2\theta + \varrho^2\sin^2\theta)^{1/2}\right]\sin\theta\mathrm{d}\theta\right\}$$

where θ is a dummy variable, $\varrho = r/R$. For evaluating the quantity $I(\arg)$ in Eq. (4) the fast Fourier transformation was applied to express $I(y)$ as a cosine expansion. The integration with respect to θ was being performed with Simpson's rule by doubling the number of intervals until the difference between the current and the previous result was below 10^{-8}. The quantity $\mathrm{d}P(\varrho)/\mathrm{d}\varrho$ was being computed by means of the same numerical formula as in [8].

6. The Kalal and Nugent method.

The cosine expansion of $I(y)$ by means of a fast Fourier transformation is used. The Eq. (2) is then expressed as

$$i(r) = \pi/2R\sum_{k=1}^{\infty} ka_k g_k(r/R) \tag{5}$$

where a_k are appopriate Fourier coefficients and $g_k(\varrho)$ are given by integrals which tend to the zero-order Bessel function of the first kind $J_0(k\Pi\varrho)$ when k become very large. The Abel inversion (5) is then calculated directly from the Fourier coefficients and the basis functions $g_k(\varrho)$. To accelerate the algorithm, the functions $g_k(\varrho)$ were precalculated for a given number of data points. The accuracy of this method is reliable, however, only on condition that the derivate vanishes near the outer radius [9].

III. NUMERICAL EXPERIMENT

Two numerical experiments were carried out. In the first experiment the above mentioned six numerical methods were tested for a different number of data points using two typical test functions. The bell-type function is given by (see Fig. 1)

$$\begin{aligned} i(r) &= 1 - 2r^2 && 0 \le r \le 1/2 \\ i(r) &= 2(1-r)^2 && 1/2 \le r \le 1. \end{aligned} \tag{6}$$

The off-axis peak-type function is given by (see Fig.2)

$$i(r) = -47.7(1-r^2)^7 + 43.5(1-r^2)^6 + 5.5(1-r^2)^5 - 0.9(1-r^2)^4. \tag{7}$$

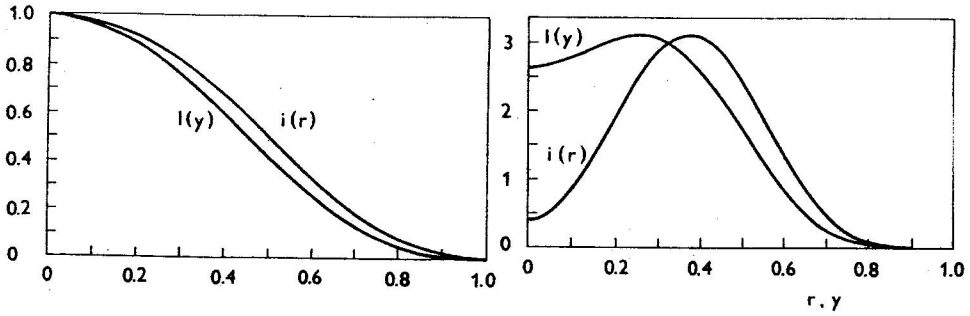

Fig. 1. Bell test function. X-axis label: r, y.

Fig. 2. Peak off-axis test function. X-axis label: r, y.

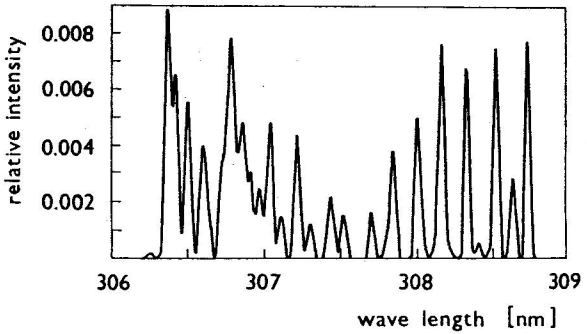

Fig. 3. A part of $A^2\Sigma \rightarrow X^2\Pi$ OH(0,0) vibrational band profile. X-axis label: Wavelenght [nm] Y-axis label: relative intensity.

First the exactly evaluated values of test functions $I(y)$ were applied, then the uniform random noise data were added. For the Frie, Vicharelli and cubic spline methods at first a simple smoothing algorithm was applied. The algorithm used the mean of the data points within a specified box size as the value at the midpoint of the box. A smoothing effect in Tatum's and Kalal's methods was obtained using only a few first Fourier coefficients. Two Fourier coefficients for the bell-type function and three for the off-axis peak-type function proved to be the best choice.

In the second numerical experiment suitable numerical methods were applid to the computation of a rotational temperature radial distribution from a theoretical vibrational band profile of the OH molecule transition $A^2\Sigma \rightarrow X^2\Pi(0,0)$. The theoretical band shape from 306.2 nm to 306.8 nm was calculated using the line parameters published by Goldman and Gillis [11]. The rotational line shape

Table 1a

Standard deviations (SD) for different data points and different noise level. S is the SD of normally distributed random noise. a) bell function

noise	intervals	Frie	spline	Cremers	Vicharelli	Kalal	Tatum
$S = 0$	10	.003243	.006356	.002242	.00756	.003319	.00231
	20	.000808	.002619	.000923	.002284	.000616	.000512
	30	.000359	.00147	.000787	.001112	.000173	.000148
	40	.000202	.000966	.000642	.000867	.000107	.000088
	50	.00013	.000696	.000574	.00086	.000067	.000051
$S = 0.01$ (1%)	10	.01696	.017268	.013964	.019267	.031244	.029869
	20	.027098	.022443	.01788	.023332	.027788	.024879
	30	.033945	.027535	.022347	.020342	.028439	.025321
	40	.040729	.033379	.021081	.02223	.030132	.027346
	50	.046509	.038038	.017008	.022176	.031629	.029594
$S = 0.05$ (5%)	10	.077713	.062726	.067749	.058843	.030859	.030308
	20	.134729	.107873	.088858	.096429	.032749	.031221
	30	.169769	.13665	.112139	.081459	.030522	.026699
	40	.203642	.166203	.105026	.085871	.027541	.023388
	50	.232545	.189734	.085217	.085259	.032732	.032642

was calculated using the formula (for example [12])

$$g(\Delta\lambda) = \frac{\alpha - (2\delta\lambda/W)^2}{\alpha + (\alpha - 2)(2\delta\lambda/W)^2}$$

were α is an arbitrary parameter chosen to equal 4 and W is the width at half maximum chosen to equal 0.04 nm [12] (which gives the band profile similar to that obtained by our PDA detector using monochromator HR 320 and the grating 2400 line s/nm, see Fig. 3).

For modelling the side-on spectra the simple forward Abel transformation algorithm was used. The algorithm is based on the same as Nestor and Olsen used for inverse transformation [1]. The bell function (6) was chosen for the radial distribution of temperature and densitz of OH molecules. The temperature distribution was transformed into the interval given by the temperature of 3000 K at the axis and 300 K at the outher radius, respectively. Experimental error was simulated adding a 1% maximum randon noise to side-on spectra. It means that the signal-to-noise ratio increases towards the outer radius.

Rotational temperatures corresponding to the band profiles obtained from a Abel transformation were determined using standard least squares procedure and compared with those from the original radial distribution.

Table 1b

Standard deviations (SD) for different data points and different noise level. S is the SD of normally distributed random noise. b) peak off-axis function

noise	intervals	Frie	spline	Cremers	Vicharelli	Kalal	Tatum
	10	.04279	.04528	.13867	.06861	.00807	.00627
	20	.01138	.00926	.00855	.03126	.00119	.00121
$S = 0$	30	.00557	.00616	.00458	.01903	.00119	.00119
	40	.00354	.00478	.00296	.01319	.00118	.00118
	50	.00262	.0038	.00233	.00986	.00117	.00117
	10	.12972	.06248	.11373	.1458	.08495	.05933
$S = 0.031$	20	.09554	.06725	.05918	.09845	.0836	.0808
(1%)	30	.11217	.08124	.06819	.09073	.08405	.08264
	40	.13336	.10067	.06513	.09912	.07728	.0728
	50	.15176	.1159	.05276	.11274	.07912	.07317
	10	.301	.15047	.15012	.28706	.21846	.25967
$S = 0.155$	20	.44577	.32849	.2784	.37734	.11564	.112
(5%)	30	.55636	.41806	.34585	.37165	.1003	.10029
	40	.66485	.51127	.32476	.42762	.11621	.10271
	50	.75758	.58501	.26372	.45812	.12535	.09752

IV. DISCUSSION-CONCLUSION

The aim of this paper is to compare some Abel transformation numerical methods and to discuss the choice of a siutable method applicable to a large amount of spectral data. The comparison is given assuming that no previous treatment of raw spectral data was made.

From the results summarized in Table 1 we can see that Kalal's and Tatum's methods give a good accuracy even when no previous smoothing is applied. Moreover, these methods involve the smoothing effect, which rapidly reduces the computational time, especially in the case of Kalal's method.

In the second numerical experiment only sufficiently quick methods were tested (Frie, Vicharelli, Kalal). The speed of Vicharelli's algorithm depens on the number of iterations. In our case five iterations proved to be sufficient to reach adequate accuracy. Increasing the number of iterations the accuracy of temperature determination is approximately the same or somewhat lower.

Table 2 shows the mean percentage deviations (MD) of calculated temperatures obtained for a set of 30 side-on spectra. Kalal's method proves to be very accurate for radial distances lower than 0.7 R ($MD \approx 1$). Beyond this limit a systematic error appears due to the increase of the signal-to-noise ratio near the outer radius which reduces the validity of the zero derivative condition. This can be, of course, substantially reduce by means of appropriate numerical filtering procedure usually used for treatment of raw spectral data.

Table 2

Percentage deviations of calculated radial temperature $\Delta T(r) = 100(T_{calc}(r) - T_{theor}(r))$ $/T_{theor}(r)$. $MD\,(n,m)$ is the mean percentage deviation, $MD(n,m) = 1/(m-n+1)\ \sum_{i=n}^{m} \Delta T(r_i)$, the noise level $(r) = 100\ S/I_{max}(r)$, where I_{max} is the maximum intensity of the corresponding side-on band profile. i and k is, respectively the number of iterations and the number of Fourier coefficients used.

r	T [K]	noise level	Frie	Vicharelli $i = 5$	Kalal $k = 3$
.000	3000	1	+14.13	+2.33	-.3
.034	2994	1	+18.92	+.08	-.05
.069	2974	1	+10.61	-2.57	+.63
.103	2942	1	-1.26	-2.01	+1.08
.138	2897	1	+6.65	-3.01	+.89
.172	2839	1	-4.7	-4.38	+.69
.207	2769	1	+.22	-2.45	+.29
.241	2685	1.1	-6.53	-4.41	+1.21
.276	2589	1.1	-.04	-2.59	+.15
.31	2480	1.1	+4.16	+.85	-.68
.345	2358	1.1	+.3	+.26	-.84
.379	2223	1.2	+5.8	-1.4	+.67
.414	2075	1.2	-6.28	-3.1	+.42
.448	1915	1.3	+5.6	+.22	-.15
.483	1741	1.3	-1.29	-4.11	-.2
.517	1559	1.4	+.55	-2.92	-.1
.552	1385	1.5	+2.23	-1.74	+1.51
.586	1225	1.7	-1.85	-4.87	+2.56
.621	1077	1.9	-.74	-.37	+2.61
.655	942	2.1	-3.51	-.65	+4.34
.69	820	2.5	+16.21	+13.77	+7.18
.724	711	3	+7.18	+5.92	+11.12
.759	615	3.8	+12.26	+11.61	+16.33
.793	531	5.1	+5.43	+3.92	+22.75
.828	461	7.3	+2.27	+1.19	+30.94
.862	403	11.6	+3.79	+1.31	+41.28
.897	358	21.6	+35.56	+32.76	+51.77
.931	326	52.6	+7.47	+94.97	+61.51
.966	306	232	-38.65	-38.97	+68.07
			$MD(1,26) = 5.48$	$MD(1,26) = 3.15$	$MD(1,26) = 5.73$
			$MD(1,15) = 5.77$	$MD(1,15) = 2.25$	$MD(1,15) = 0.55$
			$MD(4,26) = 4.30$		$MD(1,21) = 1.26$

REFERENCES

[1] Cremers, C. J., Birkebak, K. C.: Appl. Opt. *5* (1966), 1057.
[2] Frie, W.: Ann. Phys. *10* (1963), 332.
[3] Andanson, P., Chemiant, B., Halbique, A. M.: J. Phys. D: Appl. Phys. *11* (1978), 209.
[4] Sato, M.: Contrib. Plasma Phys. *25* (1985), 573.
[5] Deutsch, M., BeniaminyI.: Appl. Phys. Lett. *41* (1982), 27.
[6] Deutsch, M., Beniaminy, I.: J.Appl. Phys. Lett. *54,* (1983), 137.
[7] Vicharelli, P. A., Lapatovich, W. P.: Appl. Phys. Lett. *50,* (1987), 557.
[8] Tatum, J. B., Jaworski, W. A.: J. Quant. Spectrosc. Radiat. Transfer *38,* (1987), 319.
[9] Kalal, M., Nugent, K. A.: Appl. Opt. *27,* (1988), 1956.
[11] Goldman, A., Gillis, J. R.: J. Quant. Spectrosc. Radiat. Transfer *25* (1981), 11.
[12] Porter, R. A., Harshbarger, W. R.: J. Electrochem. Soc.: Solid State Sci. Tech. *126,* (1979), 460.

Received August 29th, 1990
Accepted for Publication April 26th, 1991

ПРИМЕНЕНИЕ НУМЕРИЧЕСКИХ МЕТОДОВ ВЫЧИСЛЕНИЯ ИНТЕГРАЛЬНОГО УРАВНЕНИЯ АБЕЛЯ В СПЕКТРОСКОПИЧЕСКИХ ДАННЫХ

В работе приводится сравнение шести нумерических методов вычисления преобразования Абеля. Обсуждается зависимость точности методов на количестве и ошибках экспериментальных данных при применении в расчетах ротационной температуры вибрационной полосы ОН молекул.